This document is published in:

Progress in Organic Coatings (2014), 77(8), 1309-1315.
DOI: 10.1016/j.porgcoat.2014.03.017

Adhesion enhancement of powder coatings on galvanised steel by addition of organo-modified silica particles

M. Puig [a,*], L. Cabedo [a], J.J. Gracenea [a], A. Jiménez-Morales [b], J. Gámez-Pérez [a], J.J. Suay [a]

[a] *Polymers and Advanced Materials Research Group (PIMA), Universitat Jaume I, Av. Vicente Sos Baynat s/n, 12071 Castellón, Spain*
[b] *Department of Materials Science and Engineering and Chemical Engineering, Universidad Carlos III, Av. Universidad 30, 28911 Leganés, Madrid, Spain*

Keywords:
Powder coating
Corrosion
Adhesion
Organosilane
Monolayer
Silica

A B S T R A C T

The addition of organo-modified silica particles (OSP) to organic monolayer coatings has been investigated as an alternative to the use of primers or surface pretreatments in galvanised steel substrates. A commercial additive consisting of trifunctional organosilane (alkyl-triethoxysilane) grafted on silica particles was directly incorporated at different concentrations (1, 2.5, 3.5 and 4.5 wt%) as an integral additive in a polyester powder coating. The OSP were characterised physicochemically by means of FTIR and TGA, and the coating formulated by DSC. The anticorrosive properties of the systems were evaluated by means of electrochemical impedance spectroscopy (EIS), showing improvements with all the formulations containing the OSP, especially in the coating with 2.5% OSP. In order to explain this behaviour, morphological (using SEM) and adhesion studies were done. The formation of agglomerates in the powder coatings was detected when the concentration was over 2.5%. There was an improvement in the adhesion of the coating to the substrate for all the samples containing the OSP but especially for that containing 2.5%. The impact resistance was increased too, especially in the formulations with 2.5% and 3.5%.

1. Introduction

Corrosion protection by powder organic coatings is considered one of the most effective and lasting mechanisms to protect metallic substrates [1,2]. However, effective protection is only possible if the coating stays bonded to the substrate during the design life of the metallic structure. In fact, conventional processes usually require an initial primer or surface pretreatment prior to applying the coating to facilitate adhesion to the substrate. This step implies an increase in the cost of corrosion protection as well as environmental problems because in many cases chromium and other heavy metals are used [3,4].

Organosilane technology emerges in the field of corrosion control of metal as a new and environmentally safer alternative to replace chromate conversion coating [5–9]. Silane adhesion promoters are silicon-based chemicals that contain two types of reactivity – inorganic and organic – in the same molecule. A typical structure is $(RO)_3Si—(CH_2)_n—R'$, where RO is a hydrolysable alkoxy group (e.g., methoxy, ethoxy and isopropoxy) that can react with various forms of hydroxyl groups present in mineral fillers or polymers and provide linkage with inorganic or organic substrates, and R′ is an organofunctional non-hydrolysable organic moiety group that provides organic compatibility or co-reacts with the coating polymer [10].

In recent years, adhesion promoters based on organosilanes have been used as a metal pretreatment and applied to metallic sub-strates [11–15]. The formation of thin silane protective films is due to two condensation reactions, one among the silanol molecules themselves (Si OH, hydrolysis products of alkoxy groups), and the other between the silanols and metal hydroxyl (Me OH) substrates to form Si O Si and Si O Me covalent bonds, respec-tively. Because of the thinness of the resulting film [16], silane films applied alone over a metallic substrate exhibit some limits when long-term protection is required, and a top organic coating to achieve high anti-corrosion performance becomes a necessity [13,17,18].

Further advances in the improvement of corrosion protection using organosilane technology consist of modifications of liquid organic coatings. Zhang et al. developed two ways by which silane monomers were incorporated into epoxy paints; they can be physically mixed with the epoxy coating [19,20] or chemically grafted to the epoxy resin before the coating formulation [21–23]. Van Ooij et al. reported an improvement by incorporating silanes directly on a polyurethane resin system to obtain a 'superprimer' with outstanding adhesion and corrosion protection properties [24]. The potential anticorrosive properties of these resin–silane

* Corresponding author.
E-mail address: puigm@uji.es (M. Puig).

combinations are based partly on the improved the adhesion between the coating and the metallic surface (Si—O—Me bonds formed as a result of reactions between silanol groups and metal hydroxyls). However, directly incorporation of silanes in powder coatings has not yet been studied. In this case, organosilane precursors grafted onto inorganic fillers seem to be a possible alternative to achieve a suitable additive for powder systems.

In this work, we assess the effect of using organo-modified silica particles (OSP) as an integral additive in polyester powder monolayer systems for anti-corrosion applications.

2. Experimental

2.1. Materials

The coatings were developed from a saturated carboxylated polyester resin of low molecular weight combined with a N,N,N′,N′-Tetrakis(2-hydroxyethyl)-hexanediamide crosslinker in a 95:5 ratio. The composition of the system was 57.7% resin, 3.3% crosslinking agent, 30% titanium dioxide, 4.7% inorganic filler (barite), 3% flow agent, 0.5% levelling agent, 0.3% degassing agent (benzoin), 0.3% polyamide wax and 0.2% Teflon wax.

The silane used in this work was a commercial additive consisting of trifunctional organosilane (alkyl-triethoxysilane) grafted to the surface of amorphous silica particles with specific surface area of 0.8812 m^2/g (reference ESQUIM DL-8302/7, supplied by Esquim S.A., Barcelona). Different concentrations of the additive (OSP) were incorporated into the formulations replacing the inorganic filler (barite) except in the reference formulation. Table 1 summarises the compositions of the samples studied in this work.

2.2. Powder coating formulations/substrate preparation

Powder coatings were premixed and hand-shacked before extrusion in a single screw extruder (Haake Rheomex 254). The extrusion temperature was set to 100 °C, the residence time was approximately 1 min and the torque generated was 20 Nm. After that, the materials were ground in a Moulinex Mill MX843 and sieved through a mesh size of 140 μm. The five different powder coatings were deposited over galvanised steel test panels from Espan color S.L., previously degreased with acetone, by means of an electrostatic gun. All the coated samples were cured at 180 °C for 15 min and the thicknesses obtained were 90 ± 10 μm.

2.3. Testing methods and equipment

2.3.1. Scanning electron microscopy (SEM)

The morphology of the coatings was observed by scanning electron microscopy (LEO 440i SEM) with digital image acquisition. The samples studied were obtained from coatings detached from their substrates after cryofracturing. The back-scattered and secondary electron images were complemented by appropriate chemical information from energy dispersive X-ray (EDS) analysis acquired as point and/or line scans.

Table 1
Composition in wt% and glass transition temperatures of the formulated coatings.

Nomenclature	Reference	1	2.5	3.5	4.5
Polyester resin	57.7	57.7	57.7	57.7	57.7
Crosslinking agent	3.3	3.3	3.3	3.3	3.3
Titanium dioxide	30.0	30.0	30.0	30.0	30.0
Barite	4.7	3.7	2.2	1.2	0.2
Flow agent	3	3	3	3	3
Levelling agent	0.5	0.5	0.5	0.5	0.5
Degassing agent	0.3	0.3	0.3	0.3	0.3
Polyamide wax	0.3	0.3	0.3	0.3	0.3
Teflon wax	0.2	0.2	0.2	0.2	0.2
OSP	0.0	1.0	2.5	3.5	4.5
T_g (°C)	63.6	64.0	63.8	63.5	63.4

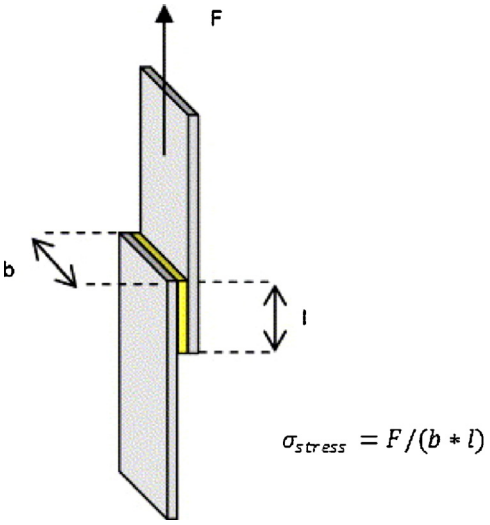

Fig. 1. Geometry of the lap joint in the adhesion test.

2.3.2. Mechanical tests

2.3.2.1. Impact resistance test. Impact testing was performed in accordance with ISO 6272-2:2002. A 1 kg dart mass is dropped down from different heights up to 1 m and impacted at the back of the painted panel, causing its rapid deformation [17,25,26]. The coating's resistance to impact may be determined from observing the film (cracked or peeled off). Five specimens of each formulation were prepared and tested.

2.3.2.2. Cross-cut test. Paint adhesion was investigated in accordance with ISO 2409:2007, using a cutter with six blades that make square lattice cuts 2 mm wide on the coating film. The cuts were made through the coating film with a steady motion using the minimal sufficient pressure on the knife. The five specimens of each formulation were visually evaluated to detect any delamination of the film. The classification of the delaminated film was based on the criteria and standard stipulated in ISO 2409:2007.

2.3.2.3. Adhesion test. A dry adhesion test was performed in accordance with ISO 4587:2003. The specimen preparation procedure for the adhesion test consisted of depositing coatings with different OSP contents between two rectangular and degreased galvanised steel substrates, as can be seen in Fig. 1 [27], and curing at 180 °C for 30 min. After the curing process, the samples were tested using an Instron Universal Test Machine 4469 H 1907 with a load cell of 50 kN and a crosshead speed of 1 mm/min. Data on load and deformation were registered. Shear stress was obtained by dividing the shear force by the cross-sectional area. Fracture modes were evaluated by means of an optical microscope. Five specimens of each formulation were prepared and tested.

2.3.3. Differential scanning calorimetry (DSC)

Differential scanning calorimetry was used to determine the glass transition temperature (T_g) of the different cured samples. Scans were performed on a Mettler DSC-821e thermal analyser calibrated using an indium standard (heat flow calibration) and an indium–lead–zinc standard (temperature calibration). Samples typically weighing 20 mg were cured in aluminium pans under nitrogen flow at a scan rate of 10 °C/min in the range of −20 to

200 °C, cooled down to −20 °C and then heated again to 200 °C at the same heating rate to obtain the T_g values.

2.3.4. FTIR spectroscopy

Fourier transform infrared (FTIR) spectra were collected for the powders using a Jasco FT/IR-6200 spectrometer in attenuated total reflection (ATR) mode. The FTIR-ATR instrument was operated in the wavenumber range of 600–4000 cm^{-1}, with a diamond/ZnSe crystal, 32 scans and resolution of 4 cm^{-1}. A background scan of clean diamond/ZnSe crystal was acquired before scanning the samples.

2.3.5. Thermogravimetric analysis (TGA)

In order to determine the influence of the OSPon the thermal stability of the formulations, thermogravimetric tests were carried out using a TG-STDA Mettler Toledo thermogravimetric analyser. Samples of approximately 15–20 mg were scanned from 50 up to 900 °C at 10 K/min. All scans were performed with a flow of 50 cm^3/min of nitrogen.

2.3.6. Electrochemical impedance spectroscopy (EIS)

The effect of adding the OSP on the anticorrosive properties of the formulated powder coatings was evaluated by EIS tests. A three-electrode system was used, in which the sample without coating acts as the working electrode, an Ag/AgCl electrode is the reference electrode and a Pt electrode is the counter-electrode. The area of the painted metal surface was defined by a cylindrical open PVC tube (9.62 cm^2 delimited circular area) that contained an aqueous electrolyte solution (3.5 wt% NaCl). EIS measurements were performed on a ZAHNER-IM6ex electrochemical workstation. A sinusoidal AC perturbation of 10 mV amplitude coupled with the open circuit potential was applied to the metal/coating system inside a Faraday cage in order to minimise external interference with the system. The EIS tests were performed in the frequency range from 100 kHz to 10 mHz. All measurements were conducted at room temperature (≈25 °C). The experimental electrochemical data were collected and analysed using the Thales software developed by ZAHNER and the Medco Assay commercial software developed by Medco S.L., respectively.

An equivalent circuit model most widely used by many authors for analyse organic paint systems to protect metals [19,21,28–30], shown in Fig. 2, was employed to analyse the EIS spectra. The circuit consisted of a working electrode (metal substrate), a reference electrode, electrolyte resistance R_S, coating pore resistance R_{po}, coating capacitance C_c, polarisation resistance R_p and double layer capacitance C_{dl}. Fitting the EIS data to the circuit by means of the Z-view software determined the values of its passive elements, which are generally assumed to be related to the corrosion properties of the system [31]. R_{po} can be related to porosity and the deterioration of the coating, C_c to the water absorption by the coating, R_p to the polarisation resistance of the interface between the coating and

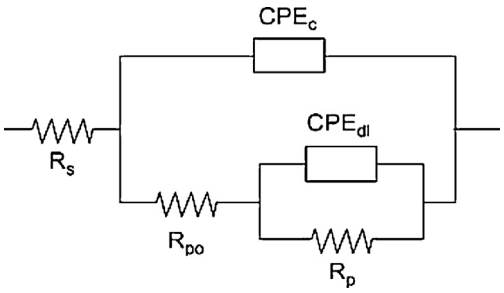

Fig. 2. Equivalent circuit used to model EIS impedance data, where passive parameters (R_s, electrolyte resistance; CPE_c, constant phase element of the coating capacitance; CPE_{dl}, constant phase element of the double layer capacitance; R_{po}, pore resistance; R_p, polarisation resistance) can be defined.

the metal substrate and C_{dl} to the disbonding of the coating and onset of corrosion at the interface [32–34]. To obtain more pre-cise fitting results, constant phase elements CPE (represented here as C) replaced capacitive elements in the equivalent circuit, giving the software values of capacitance in units of s^n/Ω together with a parameter known as "n" instead of s/Ω or F units. The chi-squared parameter of the fit was always less than 0.01.

3. Results and discussion

3.1. Characterisation of the organo-modified silica particles (OSP)

Fig. 3a shows a SEM picture of the OSP at 1000× magnifica-tion. It can be seen it is composed of small particles and aggregates with sizes on the scale of tens of microns. EDS analysis of a sin-gle particle revealed the presence of carbon in the composition, attached to the organic fraction in the additive, confirming the organo-modification of the silica particles (Fig. 3b).

FTIR spectra of the OSP are presented in Fig. 4. A broad band appears at 3378 cm^{-1} corresponding to the SiO—H stretching vibration. The alkylic chains in the organo-modifiers in the OSP can be detected by the presence of typical bands at 2950–2930 and 2850 cm^{-1}, attributed to asymmetric and symmetric CH_2 stretching, respectively. Bands corresponding to CH_2 bending vibrations are also detected with low intensity in the 1390–1400 cm^{-1} range. Detection of these bands confirms that the grafting of the silica particles was carried out predominantly by alkoxysilane-containing alkyl groups as a nonhydrolyzable organic radical. Ethoxy groups from the hydrolysable part of the alkoxysilane molecules should be detected at 1170–1160, 1100 and 1085 cm^{-1} [35]. However, these bands are masked by the broad, intense peak obtained at 1028 cm^{-1} that may ~~co~~me from Si O Si connections from the amorphous sil-ica particles, as well as those formed during the silanisation reaction with the alkoxysilane grafted onto them [36].

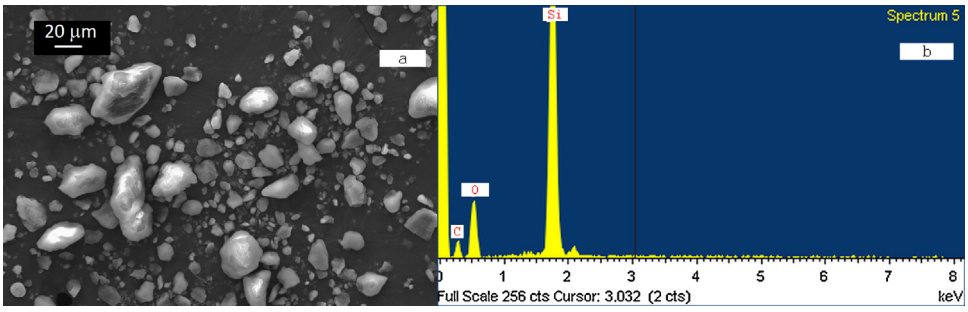

Fig. 3. (a) SEM micrograph of the supplied organo-modified silica particles (OSP) and (b) EDS analysis of OSP.

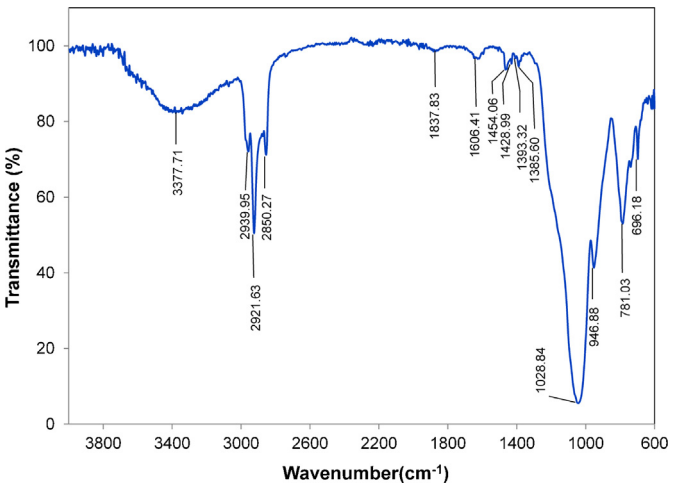

Fig. 4. FTIR spectrum of the OSP.

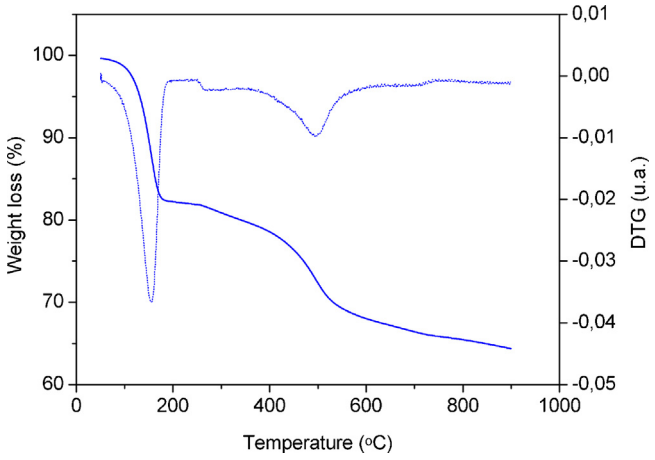

Fig. 5. TGA (—) and DTGA (- - -) curves the OSP.

TGA measurements revealed a first slight weight loss around 150 °C due to the ethoxy groups from the alkoxysilane, and a second loss that can be attributed to an oxidative thermal decomposition of non-hydrolysable alkyl chains (Fig. 5). The total weight loss was calculated at around 35%, giving insight into the degree of modification of the silica particles.

3.2. Powder coating morphological characterisation

Micrographs of the coatings containing 0, 2.5 and 4.5% OSP at 2000× magnification obtained by SEM in backscattered electron mode are shown in Fig. 6. All of them show a heterogeneous structure typical of organic powder coatings, in which three predominant phases can be identified. The brightest phase corresponds to barite particles, the darkest one corresponds to resin and the clearest particles are TiO_2 pigment perfectly dispersed in the polyester resin matrix. When the OSP are added to all the formulated systems it cannot be detected in the SEM pictures of the samples until a content of 3.5% is reached. For higher contents of OSP, the additive seems to form agglomerates, which can be above 10 μm. These agglomerates are located close to the surface of the coating (Fig. 6c). This fact may indicate the existence of a critical value (ca. 2.5%) above which the resin cannot retain a greater amount of OSP, hence forming agglomerates that are expelled to the surface, probably during the curing cycle of these paint systems.

The glass transition temperatures (T_g) obtained for the five coatings formulated with different OSP concentrations are shown in Table 1. As can be seen, there are no significant variations between them, indicating that the amount of additive incorporated does not alter the degree of crosslinking in the polyester system.

3.3. Mechanical and adhesion properties of the powder coatings

Fig. 7 shows pictures of the five samples after an impact test from a height of 100 cm with a 1 kg dart. A clear enhancement in the impact resistance compared to the reference coating can be observed with the addition of even small amounts of the OSP. Among all the systems studied, the samples with concentrations of 2.5% OSP presented only minor radial cracking in the area impacted compared with those containing either greater or smaller amounts of additive. The samples with 1% and 4.5% OSP show a fractured surface with a higher degree of delamination.

In the case of the cross-cut test, the edges of the cuts are completely smooth without detachment of flakes for all the samples except the 4.5%, which showed a small delamination in one intersection of the lattice, a defect that is detectable only if it is inspected under a magnifier.

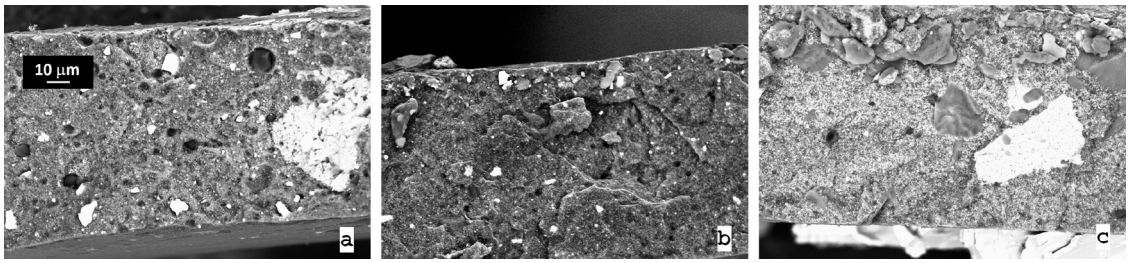

Fig. 6. SEM pictures at 2000× magnifications of coatings detached from the substrate: (a) reference, (b) 2.5% and (c) 4.5%.

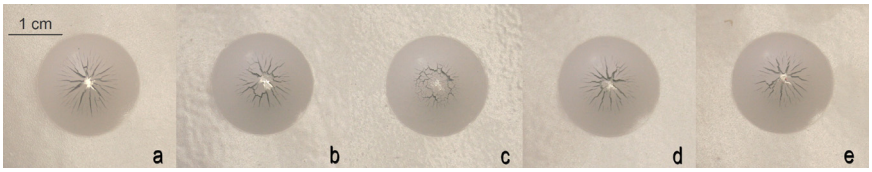

Fig. 7. Impact resistance pictures of the formulated coatings: (a) reference, (b) 1%, (c) 2.5%, (d) 3.5% and (e) 4.5%.

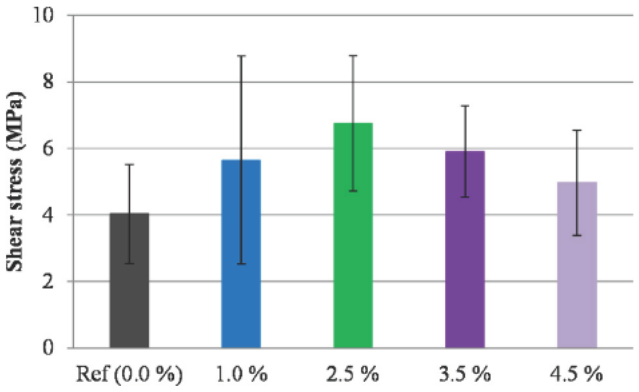

Fig. 8. Maximum shear stress of coatings formulated with different amounts of OSP in the adhesion test.

Fig. 8 shows the maximum shear stress (σ_{shear}) needed to pull apart two pieces of galvanised steel glued together by the five systems formulated in the adhesion test. The results shown indicate that the σ_{shear} was increased from the reference value when OSP were used in the formulation, and in particular from 4 to 5.6 and 6.8 MPa while modifying the reference coating with 1 and 2.5 wt% OSP, respectively. However, for higher percentages of additive the maximum shear stress decreases. The obtained standard deviation is probably due to various factors involved in the preparation of the samples, as the amount of deposited paint, or the existence of defects formed during the curing of the coating. It should be noted that adhesion of the coating to the substrate depends partly on covalent bonds formed between alkoxysilanes in the OSP and OH groups in the metallic substrate; therefore, σ_{shear} is just a measure of the adhesion when failure occurs at the interface between the resin and the substrate, i.e. it is not cohesive. To determine the failure mode of the specimens studied, the morphology of the fractured surfaces was analysed by means of an optical microscope. Fig. 9 shows one of two cross-sectional fracture areas resulting from adhesion tests corresponding to coatings containing 0, 2.5 and 4.5 wt% OSP. It can be seen that both specimens present darker areas attributed to residual paint on the substrate, and light and bright areas corresponding to the bare galvanised steel. This result indicates a mixed-mode failure that exhibits some cohesive failure and some adhesive failure. Nevertheless, in samples with 4.5% OSP, the surface is more fully covered by the coating, as can be inferred from the lack of metallic brightness on the clearer areas; therefore, the cohesive component outweighs the adhesive (Fig. 9c). The opposite is true for the reference coating (0%), where a lack of linkage along the coating-substrate interface leads to an adhesive failure (Fig. 9a). At this point, it is important to note that the fracture surface of the other side of the sample shown in Fig. 9 exhibited similar fracture morphology.

The decrease in σ_{shear} when a certain amount of OSP is exceeded can be explained by the presence of agglomerates. This fact can be clearly observed in the SEM image in Fig. 6c. The formation of additive agglomerates and their migration to the surface of the coating

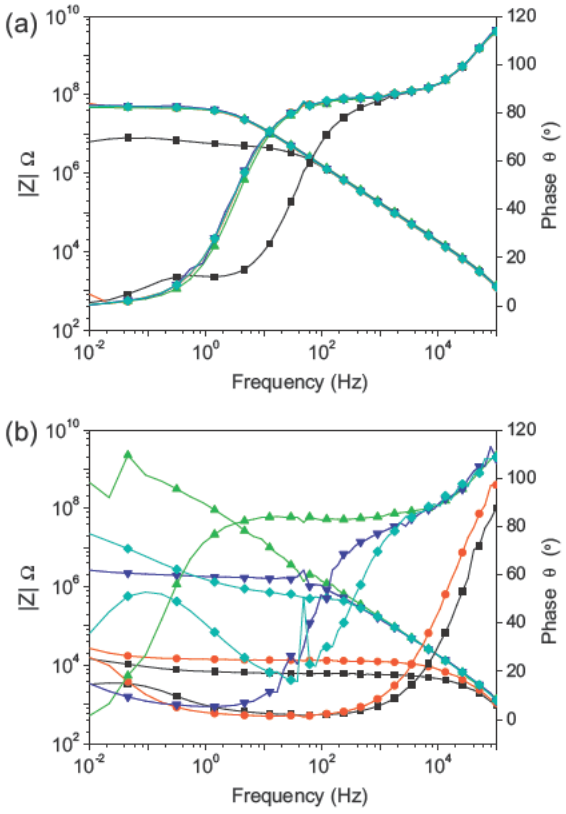

Fig. 10. Bode plots (impedance modulus vs. frequency) for coatings with different OSP concentrations: 0% (■), 1% (●), 2.5% (▲), 3.5% (▼) and 4.5% (◆) applied on metal substrate after exposure to electrolyte for 24 h (a) and 2016 h (b).

during the curing process can imply embrittlement of the paint film. Moreover, the poor dispersion may lead to a lower concentration of OSP than should be present in the coating–substrate interface, thus limiting the formation of Si—O—metal covalent bonds.

3.4. Electrochemical characterisation

Fig. 10 shows a Bode plot representing the impedance response (impedance modulus and phase angle) versus frequency for coatings formulated with different amounts of OSP after 24 h (Fig. 10a) or 2016 h (Fig. 10b) of exposure to the electrolyte. As can be seen, the coating response during short times of exposure is almost capacitive in all formulations, with almost no difference between them. However, in Fig. 10b, three very clearly differentiated trends can be observed. The first corresponds to those samples without or with just a small amount of the additive (reference 0% and 1%), which show very low impedance values and are almost resistive (phase angle with values near to 0) in all frequency ranges. The second is represented by the 2.5% coating, whose impedance module gives a straight line at low and medium frequencies, with

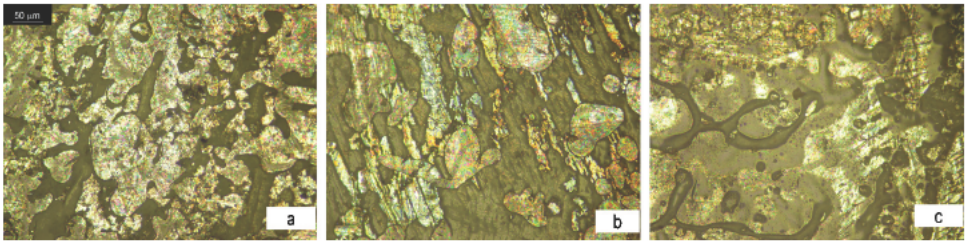

Fig. 9. Cross-sectional fracture surfaces observed via optical microscopy resulting from adhesion tests of the systems: (a) reference, (b) 2.5% and (c) 4.5%.

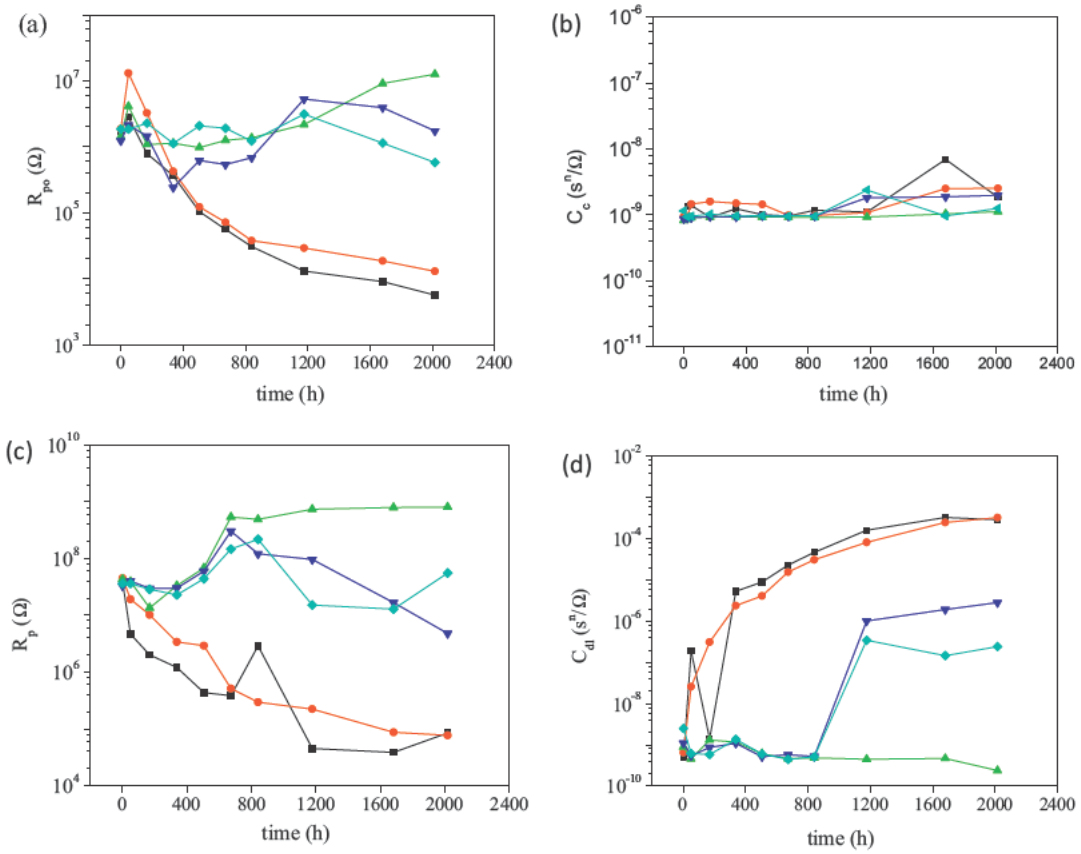

Fig. 11. Evolution of pore resistance R_{p0} (a), coating capacitance (b), polarisation resistance R_p (c) and double layer capacitance C_{dl} (d) for coatings with different OSP concentrations: 0% (■), 1% (●), 2.5% (▲), 3.5% (▼) and 4.5% (◆) after 2016 h of exposure to electrolyte.

high values of phase angle (capacitive response); and the final trend with high contents (3.5% and 4.5%) that shows an intermediate response between those of the other two trends.

Results from the EIS test were modelled with an electric equivalent circuit (Fig. 2) and the value of its passive elements determined for each exposure time. The evolution of the different parameters with immersion time (Fig. 11a–d) gave information about the anticorrosive coating properties. Pore resistance decreased continuously with exposure time in the case of samples with either 0 or 1% OSP until it had dropped more than 2.5 orders of magnitude, which is indicative of pore formation due to coating degradation (Fig. 11a). The trend in the 2.5% sample is the more stable one. The values of coating capacitance C_c present slight differences between samples and an almost constant value for the exposure time interval (Fig. 11b).

Values of polarisation resistance decreased more than 2.5 orders of magnitude for samples with 0 or 1% OSP, showing an increasing corrosion activity in these interfaces. The rest of the samples showed larger R_p values and more stable trends. Samples with 2.5, 3.5 and 4.5% OSP show a different tendency compared to the others probably due to the passivation process. This process is described by an increase of impedance values at low frequencies in Bode plot (Fig. 10b). The coating 2.5% reached the maximum value of impedance at 600 h in contact to electrolyte and it was stable until the end of the test, showing that passivation layer is stable.

Finally, samples 0 and 1.5% showed a clear coating delamination process (the double layer increased more than 5 orders of magnitude), while the 3.5% and 4.5% samples showed better performance, although after 800 h they had an increase in C_{dl} value. The 2.5% sample showed very constant values of C_{dl}, indicating the existence of an inactive interface.

The above-described results definitely show that the incorporation of OSP into the formulated systems can improve their corrosion performance, suggesting this improvement achieves an optimum value at around 2.5% by weight of the additive. This enhancement can be related to the replacement of the barite by the organically modified silica particles, which could increase the packaging of the coating leading to a more cohesive network and an improvement of the general paint properties (as can be seen in the electrochemical parameters related to the coating and to the interphase). Moreover, a second mechanism that could explain a better performance of the systems is the adhesion improvement due to the reaction of the residual unreacted hydroxyls groups of the OSP with the hydroxyls groups of metal surface.

4. Conclusions

Use of organo-modified silica particles with silanes (OSP) as an adhesion promoter in a polyester powder coating was studied. The results show that OSP incorporation leads to an improvement in the adhesion properties of the coatings, as well as in their corrosion protection, up to 2.5 wt%. Concentrations beyond 2.5 wt% entail the formation of aggregates, as observed in SEM images, leading to decreases in mechanical and electrochemical performance.

Acknowledgements

This work has been financially supported by the Spanish Ministry of the Economy and Competitiveness and the ERDF (Project IPT-020000-2010-1). The authors would like to acknowledge to MOPASA S.L. for supplying the raw materials, as well as Medco S.L.,

Raquel Oliver and José Ortega for their help in the development of this project.

References

[1] S.J. García, J. Suay, Prog. Org. Coat. 57 (2006) 273–281.
[2] S. Radhakrishnan, N. Sonawane, C.R. Siju, Prog. Org. Coat. 64 (2009) 383–386.
[3] J.W. Bibber, J. Appl. Surf. Finish. 2 (2007) 274.
[4] D.L. Correll, J. Environ. Qual. 27 (1998) 263.
[5] E.P. Plueddemann, Silane Coupling Agents, second ed., Plenum Press, New York, 1991.
[6] K.L. Mittal, Silanes and Other Coupling Agents, VSP, Utrecht, 2000.
[7] T. Peng, R. Man, J. Rare Earths 27 (2009) 159–163.
[8] S.H. Zaferani, M. Peikari, D. Zaarei, I. Danaee, J.M. Fakhraei, M. Mohammadi, Corrosion 69 (2013) 372–387.
[9] J.B. Bajat, J.P. Popí´c, V.B. Mi˘skovi´c-Stankovi´c, Prog. Org. Coat. 69 (2010) 316–321.[10] G.L. Witucki, J. Coat. Technol. 65 (1993) 57–60.
[11] F. Zucchi, A. Frignani, V. Grassi, A. Balbo, G. Trabanelli, Mater. Chem. Phys. 110 (2008) 263–268.
[12] I. De Graeve, J. Vereecken, A. Franquet, T. Van Schaftinghen, H. Terryn, Prog. Org. Coat. 59 (2007) 224–229.
[13] B. Chico, J.C. Galván, D. de la Fuente, M. Morcillo, Prog. Org. Coat. 60 (2007) 45–53.
[14] A.M. Cabral, R.G. Duarte, M.F. Montemor, M.G.S. Ferreira, Prog. Org. Coat. 54 (2005) 322–331.
[15] M. Garcia-Heras, A. Jimenez-Morales, B. Casal, J.C. Galvan, S. Radzki, M.A. Villegas, J. Alloys Compd. 380 (2004) 219–224.
[16] A. Franquet, H. Terryn, J. Vereecken, Thin Solid Films 441 (2003) 76–84.
[17] B. Díaz-Benito, F. Velasco, M. Pantoja, Prog. Org. Coat. 70 (2011) 287–292.
[18] M. Fedel, M. Olivier, M. Poelman, F. Deflorian, S. Rossi, M. Druart, Prog. Org. Coat. 66 (2009) 118–128.
[19] W. Ji, J. Hu, L. Liu, J. Zhang, C. Cao, Surf. Coat. Technol. 201 (2007) 4789–4795.
[20] L. Wu, J. Zhang, J. Hu, J. Zhang, Corros. Sci. 56 (2012) 58–66.
[21] W. Ji, J. Hu, L. Liu, J. Zhang, C. Cao, J. Adhes. Sci. Technol. 22 (2008) 77.
[22] W. Ji, J. Hu, L. Liu, J. Zhang, C. Cao, Prog. Org. Coat. 57 (2006) 439–443.
[23] W. Ji, J. Hu, J. Zhang, C. Cao, Corros. Sci. 48 (2006) 3731–3739.
[24] A. Seth, W.J. van Ooij, J. Mater. Eng. Perform. 13 (4) (2004) 468–474.
[25] S.J. Garcia, A. Serra, J. Suay, J. Appl. Polym. Sci. 105 (2007) 3097–3107.
[26] B. Pilch-Pitera, Prog. Org. Coat. 76 (2013) 33–41.
[27] S.J. García, J. Suay, Prog. Org. Coat. 57 (2006) 319–331.
[28] M.T. Rodríguez, J.J. Gracenea, A.H. Kudama, J.J. Suay, Prog. Org. Coat. 50 (2004) 62–67.
[29] C. Pérez, A. Collazo, M. Izquierdo, P. Merino, X.R. Nóvoa, Corros. Sci. 44 (2002) 481–500.
[30] D. Loveday, P. Peterson, B. Rodgers, J. Coat. Technol. 2 (2005) 22–27.
[31] F. Mansfeld, Electrochim. Acta 38 (1993) 1891–1897.
[32] A. Amirudin, D. Thieny, Prog. Org. Coat. 26 (1995) 1–28.
[33] E. Potvin, L. Brossard, G. Larochelle, Prog. Org. Coat. 31 (1997) 363–373.
[34] G.W. Walter, Corros. Sci. 26 (9) (1986) 681–703.
[35] P.J. Launer, Infrared analysis of organosilicon compounds: spectra-structure correlations I, in: B. Arkles (Ed.), Silicon Compounds: Register and Review, Petrarch Systems, Bristol, 1987, pp. 100–103.
[36] M. Lazghab, K. Saleh, P. Guigon, Chem. Eng. Res. Des. 88 (2010) 686–692.